An Energy Efficiency Analysis of Computation Offloading in MEC-Enabled IoV Networks

Tan Zheng Hui Ernest* and A S Madhukumar**
*Advanced Remanufacturing and Technology Centre, Agency for Science, Technology and Research, Singapore
**School of Computer Science and Engineering, Nanyang Technological University, Singapore
Email: ernest_tan@artc.a-star.edu.sg, asmadhukumar@ntu.edu.sg

***Abstract*—The average energy efficiency of computation offloading in multi-access edge computing (MEC) enabled Internet-of-Vehicles (IoV) networks with wired backhaul links is investigated in this paper. Specifically, the cumulative distribution function (CDF) for computation delay over wired backhaul link is derived in closed-form. The average energy efficiency of computation offloading in MEC-enabled IoV networks with wired backhaul links is derived in closed-form, and is compared against non MEC-enabled IoV networks with wired backhaul links. Numerical and simulation results show that MEC-enabled IoV networks can attain at least 10 times higher energy efficiency than non MEC-enabled IoV networks. Furthermore, we show that energy efficiency can be maximized through the proper selection of task size and transmission deadline in the MEC-enabled IoV network.**

***Index Terms*—Multi-Access Edge Computing, Computation Offloading, Energy Efficiency, Internet-of-Vehicles, Vehicular Networks.**

I. INTRODUCTION

Internet-of-Vehicles (IoV) networks are envisioned to play a critical role in meeting the demands of next-generation vehicular networks, with connected vehicles (CVs) gaining network access via road side units (RSUs) and cellular base stations (BSs) [1]. A major trend of IoV networks is multi-access edge computing (MEC), which enables tasks to be offloaded to either RSUs equipped with MEC servers or remote servers. Consequently, combining computation offloading with MEC-enabled IoV networks yields vehicular communications with lower latency and higher energy efficiency [1], [2].

In the literature, computation offloading has been extensively studied in the context of MEC-enabled cellular networks. For instance, the authors in [3] analyzed the performance of computation offloading, with closed-form expressions provided for the average delay and task completion probability in the MEC-enabled cellular network. Similarly, the authors in [4] analyzed the outage probability of an MEC-enabled wireless network for various computation offloading strategies.

In terms of IoV networks, many studies have been noted. In [2], an iterative algorithm for joint computation offloading and resource allocation was proposed to maximize the energy efficiency of MEC-enabled IoV networks. Similarly, resource allocation in IoV networks was investigated in [5] and [6], where iterative algorithms were proposed to maximize sum rate. Studies on the performance analysis of IoV networks have also been seen. For example, the performance of long-term evolution and IEEE 802.11p was studied in [7] where closed-form collision and outage probability expressions were provided. In [8], the outage probability of vehicle-to-vehicle information sharing was investigated, where closed-form outage probability expressions were derived and analyzed for general and highway scenarios.

Despite the above studies, there are still limited works on analyzing the average energy efficiency of computation offloading for MEC-enabled IoV. Specifically, most studies have focused on maximizing the instantaneous energy efficiency of computation offloading in IoV networks through resource allocation techniques or offloading optimization, e.g., in [2] and [4]. However, the design of an IoV network also impacts the resulting average energy efficiency. In particular, IoV networks with insufficient number of deployed MEC-enabled RSUs and limited wired backhaul links can experience higher overall latency and reduced energy efficiency.

To this end, the energy efficiency of computation offloading in MEC-enabled IoV networks with wired backhaul links is analyzed in this paper. Specifically, the cumulative distribution function (CDF) of the computation delay over a wired backhaul link is derived in closed-form. Based on the derived closed-form CDF expression, closed-form energy efficiency expressions are obtained for computation offloading in MEC-enabled IoV networks with wired backhaul links. Extensive analyses using non MEC-enabled IoV networks as a benchmark show that MEC-enabled IoV networks are able to achieve a substantially higher energy efficiency, which can be further maximized through appropriate task size and transmission deadline allocations.

The remainder of this paper is organized as follows. The proposed system model is introduced in Section II, with closed-form energy efficiency expressions derived Section III. Finally, the results of the numerical results are presented in Section IV before the conclusion of the paper in Section V.

II. SYSTEM MODEL

An MEC-enabled IoV network comprising M_{RSU} RSUs and M_{BS} cellular BSs is considered in this work, as seen in Fig. 1. The RSUs in the MEC-enabled IoV network each have an MEC server with a b_{MEC} GHz processor to compute tasks of size K_{size} bits received via cellular uplink transmissions from CVs with no local computing capability. Tasks from

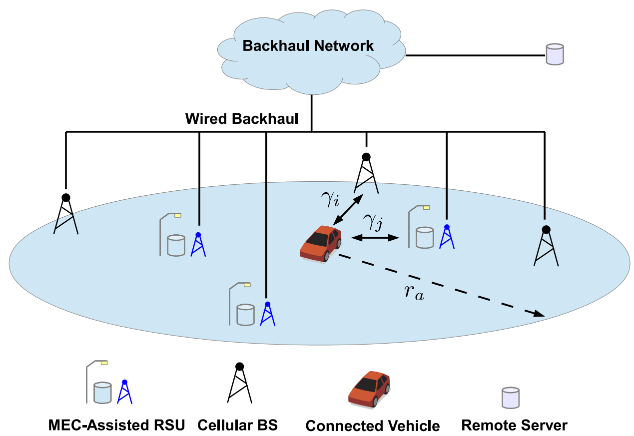

Fig. 1. A CV in an IoV network communicating with RSUs and cellular BSs.

the CVs are also offloaded to a remote server with a b_{server} GHz processor via cellular BSs with wired backhaul links, which are served by M_{GW} gateways. In particular, CVs choose the remote server for computation offloading when cellular uplink transmission between CVs and RSUs is unavailable. It is further assumed that the cellular uplink transmissions in the MEC-enabled IoV network experience Nakagami-m fading [8], and are also impaired by imperfect CSI due to Doppler shift from the mobility of CVs [5], [6].

A. Received SINR of the Typical CV

The spatial locations of RSUs and cellular BSs are modeled as binomial point processes in this study. Let the CV transmitting to either RSUs or cellular BSs be at the origin O with a communication radius of r_a. Then, the spatial locations of RSUs and cellular BSs are assumed to be uniformly distributed around a disc centered at the typical CV with radius r_a and angle $[0, 2\pi)$. Let d_i and d_j respectively denote the Euclidean distance to BS-i and RSU-j from the typical CV. Then, the probability density function (PDF) $f_{d_x}(w)$ of $d_x, x \in \{i, j\}$ is given as $f_{d_x}(w) = \frac{2w}{r_a^2}, 0 \le w \le r_a$ [9].

In the MEC-enabled IoV network, cellular BSs and RSUs with the strongest instantaneous signal-to-interference-plus-noise ratios (SINRs) are chosen by the CV for user association. Since cellular links in the MEC-enabled IoV networks are impaired by small-scale fading and Doppler shifts, channel state information (CSI) is estimated over a feedback period T [5], [6]. Let $h_x, x \in \{i, j\}$ be the channel gain between node-x and the CV, $\hat{h}_x$ be the estimated channel gain, e_x be the estimation error, and $\epsilon, 0 \le \epsilon < 1$ be the correlation coefficient between h_x and h_{x+1}. Then, using Jakes' statistical model, ϵ is defined as $\epsilon = J_0(2\pi f_d T)$ [5], [6], where J_0 is the zero-order Bessel function of the first kind [10, eq. (9.1.10)], $f_d = \frac{v f_c}{c}$ is the maximum Doppler frequency, f_c is the carrier frequency, v is the speed of the CV in m/s, and $c = 3 \times 10^8$ m/s. The first-order Gauss-Markov process is then employed to model h_x as $h_x = \epsilon \hat{h}_x + \sqrt{1-\epsilon^2} e_x$ [5], [6].

It is assumed that $|\hat{h}_x|^2$ follows the Gamma distribution with average received power $\Omega_x = \bar{P}_t \epsilon^2, x \in \{i, j\}$ and Nakagami-m fading parameter m_{Ω_x}, where $\bar{P}_t = \frac{P_t}{L_0 \eta}$ is the normalised transmit power, P_t is the transmit power of the typical CV, L_0 is the pathloss at 1 m reference distance [7], $\eta = -174 + 10\log_{10}(B_W)$ is the noise power in dBm, and B_W is the bandwidth. Likewise, $|e_x|^2, x \in \{i, j\}$ is assumed to follow the Gamma distribution with average received power $\mu_x = \bar{P}_t(1-\epsilon^2)$ and Nakagami-m fading parameter m_{μ_x}. Such an approach allows a multitude of small-scale fading effects to be modeled for both $|\hat{h}_x|^2$ and $|e_x|^2$, e.g., Rayleigh fading as assumed in [5] and [6].

Then for the typical CV, the received instantaneous SINR at BS-i (γ_i) or RSU-j (γ_j) is modeled as $\gamma_x = \frac{|\hat{h}_x|^2 d_x^{-l}}{1+|e_x|^2 d_x^{-l}}$ [5], where l is the pathloss exponent and $x \in \{i, j\}$.

B. Wired Backhaul and Processing Delay Models

For the wired backhaul link, the processing time at the gateways due to network traffic contributes to delay [11], [3]. Thus, given M_{GW} gateways and n number of hops for the wired backhaul link, the wired backhaul delay (T_{wired}) between BS-i and the remote server is modeled using the Gamma distribution [11] with shaping parameter $m_\omega = \left(1+1.28\frac{M_{\text{BS}}}{M_{\text{GW}}}\right)k_1+(n-1)k_2$, scale parameter $\theta_\omega = a + K_{\text{size}}k_3$, and average delay $\omega = \theta_\omega m_\omega$, where a, k_1, k_2, k_3 are the processing capability of the backhaul nodes.

Likewise, other computing tasks on the RSUs and the remote server also contributes to processing delays. Assuming M/M/1 queue models [3] for the remote server and RSU-j, the processing delay ($T_{\text{proc},x}$) of node-x is modeled using the exponential distribution and the PDF is given as [3, eq. (16)]:

$$f_{T_{\text{proc},x}}(t) = \left[\mu_{\text{serv},x} - \lambda_{\text{req},x}\right] \exp\left(-\left[\mu_{\text{serv},x} - \lambda_{\text{req},x}\right]t\right), \quad (1)$$

where $\mu_{\text{serv},x} = \frac{\mu_{\text{proc},x}}{K_{\text{size}}}$ is the service rate (jobs/second), $\mu_{\text{proc},x} = \frac{K_{\text{size}}}{T_{\text{comp},x}}$ is the processing rate (bits processed/second), $\lambda_{\text{req},x}$ is the request arrival rate (requests/second), $x \in \{\text{server}, j\}$. Furthermore, $T_{\text{comp},j} = \frac{K_{\text{size}}\kappa}{b_{\text{MEC}}}$ and $T_{\text{comp,server}} = \frac{K_{\text{size}}\kappa}{b_{\text{server}}}$ are respectively the computation latency of RSU-j and the remote server, and κ is the number of cycles to compute one bit [4] such that $T_{\text{proc},j}$ and $T_{\text{proc,server}}$ are the processing delays of RSU-j and the remote server, respectively.

III. Energy Efficiency Analysis of Computation Offloading

The closed-form energy efficiency expression for computation offloading in the MEC-enabled IoV network is presented in this section. The closed-form energy efficiency expression for computation offloading in non MEC-Enabled IoV networks is also presented in this section as a benchmark.

A. MEC-enabled IoV Networks

The latency taken to compute tasks from CVs in the MEC-enabled IoV network comprises the transmission latency between the typical CV and the associated RSU or cellular BS, total backhaul latency, and the computation latency to compute tasks from CVs.

Let $\phi_i = \frac{K_{\text{size}}}{B_W \log_2(1+\max_{1\le i\le M_{\text{BS}}}(\gamma_i))}$ and $\phi_j = \frac{K_{\text{size}}}{B_W \log_2(1+\max_{1\le j\le M_{\text{RSU}}}(\gamma_j))}$ respectively be the latency to transmit a task from the CV to BS-i and RSU-j. Then, the energy efficiency (η_{EE}) is defined as [4, eq. (13)]:

$$\eta_{\text{EE}} = \mathbb{P}\Big\{\phi_j \le \tau_{\text{tx}}, T_{\text{proc},j} + T_{\text{comp},j} \le \tau_{\text{comp}}\Big\} \frac{K_{\text{size}}}{\tau_{\text{tx}} P_{\text{total},j}} + \mathbb{P}\Big\{\phi_j > \tau_{\text{tx}}, \phi_i \le \tau_{\text{tx}}, T_{\text{bh}} \le \tau_{\text{comp}}\Big\} \frac{K_{\text{size}}}{\tau_{\text{tx}} P_{\text{total,server}}}, \quad (2)$$

where $\mathbb{P}\Big\{\phi_j \le \tau_{\text{tx}}, T_{\text{proc},j} + T_{\text{comp},j} \le \tau_{\text{comp}}\Big\} \frac{K_{\text{size}}}{\tau_{\text{tx}}}$ is the average rate of RSU-j, $\mathbb{P}\Big\{\phi_j > \tau_{\text{tx}}, \phi_i \le \tau_{\text{tx}}, T_{\text{bh}} \le \tau_{\text{comp}}\Big\} \frac{K_{\text{size}}}{\tau_{\text{tx}}}$ is the average rate of BS-i when , $P_{\text{total},j}$ and $P_{\text{total,server}}$ are the total power consumption to offload tasks to RSU-j and the remote server [12], [13], respectively, such that $P_{\text{total},j} = P_t + P_{\text{BB,RSU}} + P_{\text{RF,RSU}} + P_{\text{MEC}}$, $P_{\text{total,server}} = P_t + P_{\text{BB,BS}} + P_{\text{RF,BS}} + M_{\text{GW}}(P_{\text{BB,GW}} + \frac{K_{\text{size}}}{\tau_{\text{tx}}} w_{\text{bh}}) + P_{\text{server}}$, $P_{\text{BB,y}}$ is the baseband unit power consumption, $P_{\text{RF,x}}$ is the transceiver power consumption, w_{bh} is the backhaul power coefficient in Watt/bits, $y \in \{\text{RSU}, \text{BS}, \text{GW}\}$, and $x \in \{\text{RSU}, \text{BS}\}$. Furthermore, P_{MEC} is the computation power of the MEC server, P_{server} is the computation power of the remote server, τ_{tx} is the task transmission deadline, τ_{comp} is the task computation deadline, and $T_{\text{bh}} = T_{\text{wired}} + T_{\text{proc,server}} + T_{\text{comp,server}}$ is the total wired backhaul delay between BS-i and the remote server.

Evidently, obtaining the CDF of T_{bh} ($F_{T_{\text{bh}}}(\tau_{\text{comp}})$) in closed-form is a necessary step before one obtains the closed-form expression for η_{EE}. Therefore, the closed-form expression for $F_{T_{\text{bh}}}(\tau_{\text{comp}})$ is given in the following Lemma:

Lemma 1: The closed-form expression for T_{bh} is:

$$F_{T_{\text{bh}}}(\tau_{\text{comp}}) = \sum_{p=0}^{\infty} \alpha_{\omega}(p) \quad (3)$$

where $\alpha_{\omega}(p) = \frac{(-1)^p \left(\frac{m_\omega}{\omega}\right)^{m_\omega+p}}{\Gamma(m_\omega) p! (m_\omega+p)} \sum_{k=0}^{m_\omega+p} \binom{m_\omega+p}{k} \Gamma(k+1)(\tau_{\text{comp}} - T_{\text{comp,server}})^{m_\omega+p-k} \left(\frac{-1}{\mu_{\text{serv,server}} - \lambda_{\text{req,server}}}\right)^k$ and $\Gamma(\cdot)$ is the Gamma function.

Proof: The proof is given in Appendix A. ■

Based on Lemma 1, the closed-form expression for η_{EE} is given in the following Theorem:

Theorem 1: The closed-form expression for η_{EE} is:

$$\eta_{\text{EE}} = \left[1 - \left(\sum_{p=0}^{\infty} \alpha_{\Omega_j}(p)\right)^{M_{\text{RSU}}}\right] \frac{F_{T_{\text{proc},j}}(\tau_{\text{comp}}) K_{\text{size}}}{\tau_{\text{tx}} P_{\text{total},j}} + \left(\sum_{p=0}^{\infty} \alpha_{\Omega_j}(p)\right)^{M_{\text{RSU}}} \left[1 - \left(\sum_{p=0}^{\infty} \alpha_{\Omega_i}(p)\right)^{M_{\text{BS}}}\right] \frac{F_{T_{\text{bh}}}(\tau_{\text{comp}}) K_{\text{size}}}{\tau_{\text{tx}} P_{\text{total,server}}}, \quad (4)$$

where $\alpha_{\Omega_x}(p) = \frac{(-1)^p \left(\frac{m_{\Omega_x} \gamma_{\text{tx}}}{\Omega_x}\right)^{m_{\Omega_x}+p}}{\Gamma(m_{\Omega_x}) p! (m_{\Omega_x}+p)} \sum_{k=0}^{m_{\Omega_x}+p} \binom{m_{\Omega_x}+p}{k} \left(\frac{\Omega_x}{m_{\Omega_x}}\right)^k \times \frac{\Gamma(m_{\Omega_x}+k)}{\Gamma(m_{\Omega_x})} \delta_{m_{\Omega_x}}(p,k)$, $\delta_{m_{\Omega_x}}(p,k) = \frac{2(r_a)^{l(m_{\Omega_x}+p-k)}}{l(m_{\Omega_x}+p-k)+2}$, $\gamma_{\text{tx}} = 2^{\frac{K_{\text{size}}}{\tau_{\text{tx}} B_W}} - 1$, and $F_{T_{\text{proc},j}}(\tau_{\text{comp}}) = 1 - \exp\big(-\big[\mu_{\text{serv},j} - \lambda_{\text{req},j}\big]\big[\tau_{\text{comp}} - T_{\text{comp},j}\big]\big)$ is the CDF of $T_{\text{proc},j}$.

Proof: The proof is given in Appendix B. ■

The closed-form expression in (4) shows that the energy efficiency of MEC-enabled IoV networks is highly dependent on the quality of cellular uplink transmissions, processing

TABLE I
DEFAULT SIMULATION PARAMETERS

Description	Value(s)
Transmissions Parameters	$K_{\text{size}} = 9$ MB, $M_{\text{RSU}} = 5$, $M_{\text{BS}} = 3$ $P_t = 20$ dBm [8], $l = 2$ [8] $L_0 = 47.86$ dB [7], $\tau_{\text{tx}} = 3$ $f_c = 5.9$ GHz [7], $B_{\text{w}} = 10$ MHz [7] $T = 0.5$ ms [6], $r_{\text{a}} = 500$m
Power Consumption Parameters	$P_{\text{BB,BS}} = 29.6$W, $P_{\text{RF,BS}} = 12.9$W $P_{\text{BB,RSU}} = 1$W, $P_{\text{RF,RSU}} = 3$W $P_{\text{MEC}} = 0.2$W, $P_{\text{BB,GW}} = 29.6$W $P_{\text{server}} = 0.2$W
Server and Gateway Parameters	$b_{\text{server}} = b_{\text{MEC}} = 9$ GHz, $n = 3$ $\kappa = 10$ cycles/bit, $\tau_{\text{comp}} = 8$ $M_{\text{GW}} = 2$, $w_{\text{bh}} = 5 \times 10^{-7}$Watt/bit $k_1 = 1$, $k_2 = 2$, $k_3 = 10^{-8}$, $a = 10^{-5}$ $\lambda_{\text{req},j} = \lambda_{\text{req,server}} = 2$
Nakagami-m Fading Parameters	$m_{\Omega_x} = m_{\mu_x} = 2, x \in \{i, j\}$

delay at the RSUs and remote server, the wired backhaul delay, and the size of tasks to be offloaded. Therefore, high energy efficiency in MEC-enabled IoV networks is a function of P_t, τ_{tx}, and K_{size}.

B. Non MEC-Enabled IoV Networks

The latency taken to compute tasks from CVs in a non MEC-enabled IoV network comprises the transmission latency between the typical CV and the associated cellular BS, total backhaul latency, and the computation latency at the remote server to compute tasks from CVs. Then, based on (2), the energy efficiency of a non MEC-enabled IoV network ($\eta_{\text{EE,Non MEC}}$) is defined as [4, eq. (13)]:

$$\eta_{\text{EE,Non MEC}} = \mathbb{P}\Big\{\phi_i \le \tau_{\text{tx}}, T_{\text{bh}} \le \tau_{\text{comp}}\Big\} \frac{K_{\text{size}}}{\tau_{\text{tx}} P_{\text{total,server}}}. \quad (5)$$

The closed-form expression for $\eta_{\text{EE,non MEC}}$ is thus given in the following Theorem:

Theorem 2: The closed-form expression for $\eta_{\text{EE,non MEC}}$ is:

$$\eta_{\text{EE,non MEC}} = \left[1 - \left(\sum_{p=0}^{\infty} \alpha_{\Omega_i}(p)\right)^{M_{\text{BS}}}\right] \frac{F_{T_{\text{bh}}}(\tau_{\text{comp}}) K_{\text{size}}}{\tau_{\text{tx}} P_{\text{total,server}}}. \quad (6)$$

Proof: The expression in (6) is obtained using the same approach in Appendix B. ■

Similar to (4), the closed-form expression in (6) shows that the energy efficiency of MEC-enabled IoV networks is highly dependent on the quality of cellular uplink transmissions, the wired backhaul delay, and the size of tasks to be offloaded. Therefore, obtaining high energy efficiency in non MEC-enabled IoV networks is a function of P_t, τ_{tx}, and K_{size}.

IV. NUMERICAL RESULTS

In this section, numerical results pertaining to the energy efficiency of MEC-enabled IoV networks are presented, with Monte Carlo simulations conducted with 10^4 samples using the default simulation parameters in Table I. Numerical results are also provided for non MEC-enabled IoV networks as a benchmark.

Starting with Fig. 2, the closed-form expression for $F_{T_{\text{bh}}}(\tau_{\text{comp}})$ provided in (3) is compared with simulations

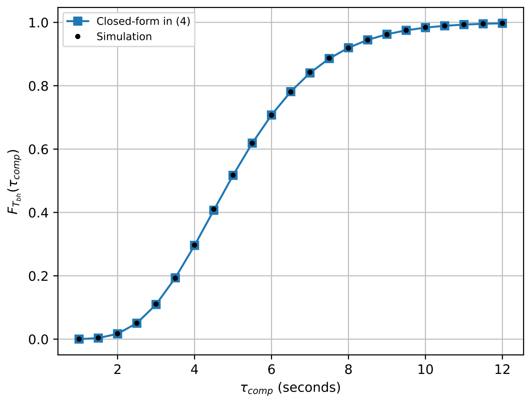

Fig. 2. Validation of $F_{T_{\mathrm{bh}}}(\tau_{\mathrm{comp}})$ provided in (3) with simulation.

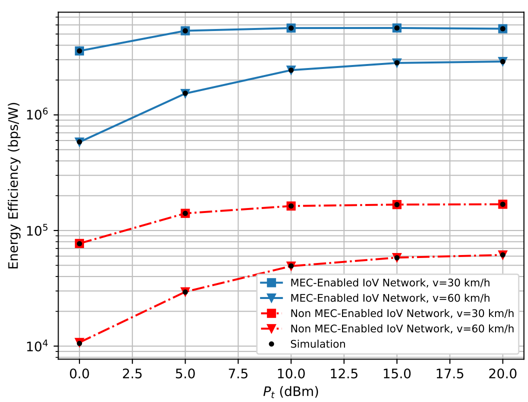

Fig. 3. The impact of P_t on energy efficiency in non MEC-enabled and MEC-enabled IoV networks.

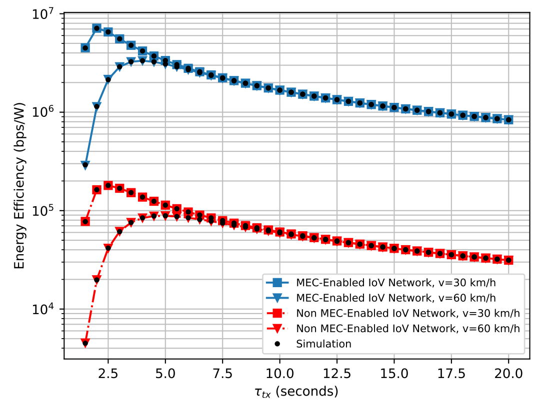

Fig. 4. The impact of τ_{tx} on energy efficiency in non MEC-enabled and MEC-enabled IoV networks.

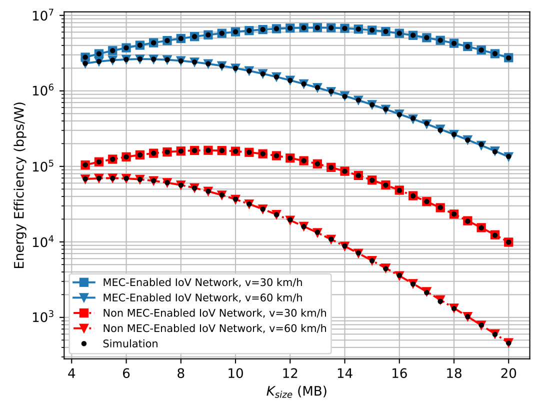

Fig. 5. The impact of K_{size} on energy efficiency in non MEC-enabled and MEC-enabled IoV networks.

for accuracy validation. In particular, (3) is validated as it matches closely with the simulations. The impact of P_t is shown in Fig. 3. It is observed that the energy efficiency of the MEC-enabled (η_{EE}) and non MEC-enabled ($\eta_{\mathrm{EE,non\ MEC}}$) IoV networks plateaus as the transmit power P_t is increased when the typical CV is traveling at high (v = 60 km/h) and low (v = 30 km/h) speed. It is also observed that η_{EE} and $\eta_{\mathrm{EE,non\ MEC}}$ are higher when v = 60 km/h as compared to v = 30 km/h. Such observations are due to the fact that η_{EE} and $\eta_{\mathrm{EE,non\ MEC}}$ become interference-limited due to CSI estimation errors, which increases proportionally to CV mobility. In addition, it is seen in Fig. 3 that $\eta_{\mathrm{EE}} > \eta_{\mathrm{EE,non\ MEC}}$ and this is due to the benefits of lower transmission and computation latencies brought about by the MEC-enabled RSUs.

The impact of τ_{tx} and K_{size} are shown in Fig. 4 and Fig. 5, respectively. In Fig. 4, it is observed that η_{EE} and $\eta_{\mathrm{EE,non\ MEC}}$ peak at τ_{tx} = 2 seconds and τ_{tx} = 2.5 seconds, respectively, when v = 30 km/h. When the typical CV travels at higher speeds, i.e., v = 60 km/h, it is seen that η_{EE} and $\eta_{\mathrm{EE,non\ MEC}}$ peak at τ_{tx} = 3.5 seconds and τ_{tx} = 4.5 seconds, respectively. Similarly in Fig. 5, it is observed that η_{EE} and $\eta_{\mathrm{EE,non\ MEC}}$ peak at K_{size} = 13 MB and K_{size} = 9MB, respectively, when v = 30 km/h. As the typical CV travels at a higher speed, i.e., v = 60 km/h, it is seen that η_{EE} and $\eta_{\mathrm{EE,non\ MEC}}$ peak at K_{size} = 6.5 MB and K_{size} = 5.5MB, respectively.

The peaks in Fig. 4 and Fig. 5 are due to the fact that an optimal transmission rate is identified as τ_{tx} and K_{size} are varied. Furthermore, the trends in Fig. 4 and Fig. 5 are further influenced by CV mobility and the lower task transmission latency provided by MEC-enabled RSUs. In particular, a typical CV traveling higher speeds evoke a higher CSI estimation error which in turn affects the cellular uplink transmission in MEC-enabled and non MEC-enabled IoV networks. As a result, MEC-enabled are able to support higher K_{size} and lower τ_{tx} requirements than non MEC-enabled IoV networks when v = 30 km/h. Furthermore, Fig. 4 and Fig. 5 shows that selecting the appropriate τ_{tx} and K_{size} is crucial in maximizing energy efficiency in both MEC-enabled and non MEC-enabled IoV networks.

V. Conclusion

The average energy efficiency of computation offloading in MEC-enabled IoV networks with wired backhaul links is analyzed in this paper. In particular, the computation delay CDF over a wired backhaul link is derived in closed-form. Using the computation delay CDF, a closed-form expression for the average energy efficiency of computation offloading in MEC-enabled IoV networks is obtained. The closed-form energy efficiency expression for computation offloading in non MEC-enabled IoV networks is also derived as a comparison.

The numerical analysis and related simulation studies indicate that the MEC-enabled IoV network yields at least 10 times higher energy efficiency when compared to a non MEC-enabled IoV network. The average energy efficiency is also shown to be maximized when selecting appropriate values for task size and transmission deadline in the MEC-enabled IoV network.

Appendix A
Proof of (3)

We start by letting $\mathbb{P}\{T_{\text{wired}} \leq \tau_{\text{comp}}\}$ be the CDF of T_{wired}. Then, the CDF of T_{bh} ($F_{T_{\text{bh}}}(\tau_{\text{comp}})$) can be expressed as:

$$F_{T_{\text{bh}}}(\tau_{\text{comp}}) = \mathbb{P}\Big\{T_{\text{wired}} \leq \tau_{\text{comp}} - T_{\text{proc,server}} - T_{\text{comp,server}}\Big\} = \mathbb{E}\Big\{F_{T_{\text{wired}}}\big(\tau_{\text{comp}} - T_{\text{proc,server}} - T_{\text{comp,server}}\big)\Big\}, \quad (7)$$

where $\mathbb{E}\{\bullet\}$ is the expectation operator. From [14, Table I], $F_{T_{\text{wired}}}\big(\tau_{\text{comp}} - T_{\text{proc,server}} - T_{\text{comp,server}}\big)$ conditioned on $T_{\text{proc,server}}$, i.e., $F_{T_{\text{wired}}|T_{\text{proc,server}}}\big(\tau_{\text{comp}} - T_{\text{proc,server}} - T_{\text{comp,server}}\big)$ can be written as:

$$\begin{aligned} &F_{T_{\text{wired}}|T_{\text{proc,server}}}\big(\tau_{\text{comp}} - T_{\text{proc,server}} - T_{\text{comp,server}}\big) \\ &= \sum_{p=0}^{\infty} \frac{(-1)^p \left(\frac{m_\omega}{\omega}\right)^{m_\omega+p}}{\Gamma(m_\omega)p!(m_\omega+p)} \times \big(\tau_{\text{comp}} - T_{\text{proc,server}} - T_{\text{comp,server}}\big)^{m_\omega+p} \\ &= \sum_{p=0}^{\infty} \frac{(-1)^p \left(\frac{m_\omega}{\omega}\right)^{m_\omega+p}}{\Gamma(m_\omega)p!(m_\omega+p)} \sum_{k=0}^{m_\omega+p} \binom{m_\omega+p}{k} \times (-1)^k (\tau_{\text{comp}} - T_{\text{comp,server}})^{m_\omega+p-k} \big(T_{\text{comp,server}}\big)^k. \end{aligned} \quad (8)$$

Finally, $F_{T_{\text{bh}}}\big(\tau_{\text{comp}}\big)$ can be written in closed-form as [14, Table II]:

$$\begin{aligned} F_{T_{\text{bh}}}\big(\tau_{\text{comp}}\big) &= \sum_{p=0}^{\infty} \frac{(-1)^p \left(\frac{m_\omega}{\omega}\right)^{m_\omega+p}}{\Gamma(m_\omega)p!(m_\omega+p)} \sum_{k=0}^{m_\omega+p} \binom{m_\omega+p}{k} \times (-1)^k (\tau_{\text{comp}} - T_{\text{comp,server}})^{m_\omega+p-k} \mathbb{E}\Big\{\big(T_{\text{comp,server}}\big)^k\Big\} \\ &= \sum_{p=0}^{\infty} \frac{(-1)^p \left(\frac{m_\omega}{\omega}\right)^{m_\omega+p}}{\Gamma(m_\omega)p!(m_\omega+p)} \sum_{k=0}^{m_\omega+p} \binom{m_\omega+p}{k} \Gamma(k+1) \times (\tau_{\text{comp}} - T_{\text{comp,server}})^{m_\omega+p-k} \left(\frac{-1}{\mu_{\text{serv,server}} - \lambda_{\text{req,server}}}\right)^k \\ &= \sum_{p=0}^{\infty} \alpha_\omega(p). \end{aligned} \quad (9)$$

This completes the proof.

Appendix B
Proof of (4)

We start by rewriting (2) as:

$$\begin{aligned} \eta_{\text{EE}} = &\left[1 - \left(\mathbb{P}\Big\{\gamma_j \leq \gamma_{\text{tx}}\Big\}\right)^{M_{\text{RSU}}}\right] \frac{F_{T_{\text{proc},j}}(\tau_{\text{comp}})K_{\text{size}}}{\tau_{\text{tx}} P_{\text{total},j}} \\ &+ \left(\mathbb{P}\Big\{\gamma_j \leq \gamma_{\text{tx}}\Big\}\right)^{M_{\text{RSU}}} \left[1 - \left(\mathbb{P}\Big\{\gamma_i \leq \gamma_{\text{tx}}\Big\}\right)^{M_{\text{BS}}}\right] \times \frac{F_{T_{\text{bh}}}\big(\tau_{\text{comp}}\big)K_{\text{size}}}{\tau_{\text{tx}} P_{\text{total,server}}}, \end{aligned} \quad (10)$$

where $F_{T_{\text{proc},j}}(\tau_{\text{comp}})$ is easily evaluated in closed-form as $F_{T_{\text{proc},j}}(\tau_{\text{comp}}) = 1 - \exp\big(-\big[\mu_{\text{serv},j} - \lambda_{\text{req},j}\big]\big[\tau_{\text{comp}} - T_{\text{comp},j}\big]\big)$.

Applying the approach in [9, Lemma 1] and making the necessary substitutions from [14, Table I] and [14, Table II], $\mathbb{P}\Big\{\gamma_x \leq \gamma_{\text{tx}}\Big\}, x \in \{i, j\}$ is evaluated as:

$$\begin{aligned} \mathbb{P}\Big\{\gamma_x \leq \gamma_{\text{tx}}\Big\} &= \sum_{p=0}^{\infty} \frac{(-1)^p \left(\frac{m_{\Omega_x}\gamma_{\text{tx}}}{\Omega_x}\right)^{m_{\Omega_x}+p}}{\Gamma(m_{\Omega_x})p!(m_{\Omega_x}+p)} \sum_{k=0}^{m_{\Omega_x}+p} \binom{m_{\Omega_x}+p}{k} \times \left(\frac{\Omega_x}{m_{\Omega_x}}\right)^k \frac{\Gamma(m_{\Omega_x}+k)}{\Gamma(m_{\Omega_x})} \mathbb{E}\Big\{(d_x)^{l(m_{\Omega_x}+p-k)}\Big\} \\ &= \sum_{p=0}^{\infty} \alpha_{\Omega_x}(p) \end{aligned} \quad (11)$$

Substituting the closed-form expression for $F_{T_{\text{proc},j}}(\tau_{\text{comp}})$, along with (9) and (11) into (10) yields (4). This completes the proof.

References

[1] H. Zhou, W. Xu, J. Chen, and W. Wang, "Evolutionary V2X technologies toward the Internet of Vehicles: Challenges and Opportunities," *Proc. IEEE*, vol. 108, no. 2, pp. 308–323, Feb. 2020.

[2] S. Raza, S. Wang, M. Ahmed, M. R. Anwar, M. A. Mirza, and W. U. Khan, "Task offloading and resource allocation for IoV using 5G NR-V2X communication," *IEEE Internet Things J.*, July 2022.

[3] H. Hu, J. Zhang, Y. Jiang, Z. Li, Q. Chen, and J. Zhang, "Computation Offloading Analysis in Clustered Fog Radio Access Networks With Repulsion," *IEEE Trans. Veh. Technol.*, vol. 70, no. 10, pp. 10 804–10 819, 2021.

[4] X. Lai, J. Xia, L. Fan, T. Q. Duong, and A. Nallanathan, "Outdated Access Point Selection for Mobile Edge Computing With Cochannel Interference," *IEEE Trans. Veh. Technol.*, July 2022.

[5] L. Liang, J. Kim, S. C. Jha, K. Sivanesan, and G. Y. Li, "Spectrum and power allocation for vehicular communications with delayed CSI feedback," *IEEE Wireless Commun. Lett.*, vol. 6, no. 4, pp. 458–461, Aug. 2017.

[6] X. Li, L. Ma, Y. Xu, and R. Shankaran, "Resource allocation for D2D-based V2X communication with imperfect CSI," *IEEE Internet Things J.*, vol. 7, no. 4, pp. 3545–3558, April 2020.

[7] A. Bazzi, B. M. Masini, A. Zanella, and I. Thibault, "On the performance of IEEE 802.11 p and LTE-V2V for the cooperative awareness of connected vehicles," *IEEE Trans. Veh. Technol.*, vol. 66, no. 11, pp. 10 419–10 432, Nov. 2017.

[8] C. Jiang, H. Zhang, Z. Han, Y. Ren, V. C. Leung, and L. Hanzo, "Information-sharing outage-probability analysis of vehicular networks," *IEEE Trans. Veh. Technol.*, vol. 65, no. 12, pp. 9479–9492, Dec. 2016.

[9] T. Z. H. Ernest, A. S. Madhukumar, R. P. Sirigina, and A. K. Krishna, "Hybrid-Duplex Communications for Multi-UAV Networks: An Outage Probability Analysis," *IEEE Commun. Lett.*, vol. 23, no. 10, pp. 1831–1835, October 2019.

[10] M. Abramowitz and I. Stegun, "Handbook of mathematical functions with formulas, graphs, and mathematical tables (applied mathematics series 55)," *National Bureau of Standards, Washington, DC*, 1964.

[11] G. Zhang, T. Q. Quek, M. Kountouris, A. Huang, and H. Shan, "Fundamentals of heterogeneous backhaul design—Analysis and optimization," *IEEE Trans. Commun.*, vol. 64, no. 2, pp. 876–889, 2016.

[12] D. Liu and C. Yang, "Energy efficiency of downlink networks with caching at base stations," *IEEE J. Sel. Areas Commun.*, vol. 34, no. 4, pp. 907–922, April 2016.

[13] G. Auer, V. Giannini, C. Desset, I. Godor, P. Skillermark, M. Olsson, M. A. Imran, D. Sabella, M. J. Gonzalez, O. Blume *et al.*, "How much energy is needed to run a wireless network?" *IEEE Wireless Commun.*, vol. 18, no. 5, pp. 40–49, October 2011.

[14] N. B. Rached, A. Kammoun, M.-S. Alouini, and R. Tempone, "A unified moment-based approach for the evaluation of the outage probability with noise and interference," *IEEE Trans. Wireless Commun.*, vol. 16, no. 2, pp. 1012–1023, 2017.